Engineering Structures 30 (2008) 3555–3565

Contents lists available at ScienceDirect

Engineering Structures

journal homepage: www.elsevier.com/locate/engstruct

Wind-induced interaction of a non-uniform tuned liquid column damper and a structure in pitching motion

Jong-Cheng Wu [a,*], Yen-Po Wang [b], Chien-Liang Lee [b], Pei-Hsuan Liao [a], Yi-Hsuan Chen [b]

[a] Department of Civil Engineering, Tamkang University, Taipei, Taiwan

[b] Department of Civil Engineering, National Chiao Tung University, Hsinchu, Taiwan

ARTICLE INFO

Article history:
Received 20 November 2007
Received in revised form
19 May 2008
Accepted 20 May 2008
Available online 9 July 2008

Keywords:
Tuned liquid column damper (TLCD)
Non-uniform cross-section
Pitching interaction
Head loss coefficient
Forced vibration

ABSTRACT

Wind-induced interaction between a tuned liquid column damper (TLCD) and a structure (bridge deck) in pitching motion is investigated both theoretically and experimentally. Non-uniform cross-sections in TLCDs are considered in general. Theoretically, the interacted equations of motion under wind excitation were derived for a single-degree-of-freedom rotational structure equipped with a TLCD based on energy principles. An addition term, which had never been revealed in existing literature, was discovered. The second part in this study was to demonstrate the existence of this additional term through experimental verification. This task was carried out by conducting large scale tests on the system of a TLCD on a rotational structure (which is a spring-constrained steel beam pivoted at mid-span) and by making comparisons between the experimental and analytical responses of the interacted structure subjected to harmonic loading. To obtain all necessary parameters for computing the analytical responses in the interaction, the individual identification of the properties of the TLCD and structure using free vibration and forced vibration techniques was also performed. Comparison results show that analytical responses with the additional term included can represent the actual interaction more closely than those without the additional term. Therefore, the inclusion of the additional term in pitching interaction equations is essential.

1. Introduction

In recent years, the aesthetical consideration accompanied with advancement in material and construction technology has facilitated a new generation of bridges with lighter weights and longer spans. The down side is the high susceptibility of their response to wind load. Thus, for structures such as these, it is becoming more necessary to use control devices for the sake of vibration suppression. Among many varieties of choices for control devices, the tuned liquid column damper (TLCD) is a good candidate, though most of the applications today are on buildings which are subjected to horizontal motion. The original idea of TLCD was developed specifically for suppression of horizontal vibration by Sakai et al. [1]. In terms of advantages over other types of energy-dissipating dampers, the properties of TLCD (such as the natural frequency and damping) can be reliably and precisely determined from the length of the liquid column and the orifice size in the liquid column. As can be seen from the literature, many researchers, namely Xu et al. [2], Hitchcock et al. [3] and Balendra et al. [4], have verified its effectiveness for suppressing wind-induced responses, among whom Hitchcock et al. [3] even investigate a general type of TLCDs that have non-uniform cross-sections in the horizontal and vertical columns, termed as liquid column vibration absorbers (LCVA). The optimal parameters for TLCD designs were also given in Gao et al. [5], Chang and Hsu [6] and Chang [7], and later convenient guidelines, such as the design tables and empirical formula of head loss coefficients, for practical design were summarized by Wu et al. [8].

For suppressing wind-induced pitching (torsional) motion of bridges, the interaction mechanism of TLCDs and structures in pitching motion will have to be addressed. As we know, using tuned mass dampers (TMD) for controlling the pitching motion of bridges is to simply configure vertical TMDs on the two sides of the bridge deck tuned to the torsional mode (e.g., Kwon and Park [9]). The mechanism involved is basically the same as that in the application to control torsional responses of buildings (Pansare and Jangid [10], Jangid and Datta [11]). Unfortunately, this analogy can not apply to TLCD because of the fluid inside. The TLCDs for controlling bridge decks will have to move rotationally together with the bridge deck. For simplicity, the interacted equations of motion of a single-degree-of-freedom (SDOF) rotational structure equipped with a TLCD with uniform cross-sections has been first presented by Xue et al. [12] and later the optimal parameters for

* Corresponding author. Tel.: +886 2 26215656x2758; fax: +886 2 26209747.
E-mail address: joncheng@mail.tku.edu.tw (J.-C. Wu).

0141-0296/$ – see front matter © 2008 Elsevier Ltd. All rights reserved.
doi:10.1016/j.engstruct.2008.05.029

Nomenclature

A_h cross-section area in the horizontal column of a TLCD;
A_v cross-section area in the vertical column of a TLCD;
e vertical distance between the rotational center of the structure and the horizontal liquid column in a TLCD;
g acceleration due to gravity;
h integrating variable indicated in Fig. 1;
$J_\alpha, C_\alpha, K_\alpha$ structural mass moment of inertia, damping and stiffness constants;
$k = \omega/\omega_d$ ratio of the excitation frequency versus TLCD natural frequency (excitation frequency ratio);
$L = 2L_v + L_h$ total length of the liquid column in a TLCD;
$L_e = 2L_v + \nu L_h$ effective length of the liquid column in a TLCD;
L_h horizontal column length in a TLCD;
L_v vertical column length in a TLCD;
l integrating variable indicated in Fig. 1;
$M(t)$ external moment acting on the structure;
$\hat{M}(\hat{t}) = MT_d^2/J_\alpha$ nondimensional $M(t)$;
$\hat{M}_0$ amplitude of $\hat{M}(\hat{t})$ in harmonic motion;
$m = \nu p/(\nu + p(1-\nu))$ parameter related to ν and p;
$n = p/(1 - p(1-\nu))$ parameter related to ν and p;
$p = L_h/L$ ratio of the horizontal length to total length of the liquid column;
$Q_{nc,\alpha}$ (or $Q_{nc,y}$) non-conservative force in the direction of generalized coordinates α (or y);
S_1 (or S_2) distance between the structural rotational center and the center of the left (or right) vertical liquid column, as indicated in Fig. 1;
T kinetic energy;
$T_d = 2\pi\sqrt{L_e/2g}$ natural period of a TLCD;
$T_{\alpha\hat{M}}$ (or $T_{\hat{y}\hat{M}}$) frequency response function of α (or $\hat{y}$) induced by $\hat{M}$;
t time;
$\hat{t} = t/T_d$ nondimensional time;
V potential energy;
y liquid displacement in a TLCD;
$\hat{y} = y/L_h$ non-dimensional liquid displacement in a TLCD;
$\hat{y}_0$ amplitude of $\hat{y}$ in harmonic motion;
α rotational angle of a structure;
α_0 amplitude of α in harmonic motion;
$\beta_1 = \omega_\alpha/\omega_d$ frequency tuning ratio of the structure versus TLCD;
ρ fluid density;
φ_y amplitude of y in harmonic liquid motion;
$\varphi_{\hat{y}} = \varphi_y/L_h$ non-dimensional amplitude of y in harmonic liquid motion;
ψ blocking ratio of the orifice in a TLCD;
$\mu = J_d/J_\alpha$ ratio of mass moment of inertia between the liquid and structure;
$\nu = A_v/A_h$ cross-section ratio of the vertical column versus horizontal column;
ω excitation frequency;
$\omega_d = \sqrt{2g/L_e}$ natural frequency of a TLCD;
$\omega_\alpha = \sqrt{K_\alpha/J_\alpha}$ natural frequency of a structure
$\xi = C_\alpha/2J_\alpha\omega_\alpha$ damping ratio of a structure;
η head loss coefficient

design under a harmonic type or white noise type of wind loading was successively investigated and presented in Xue et al. [13] and Taflanidis et al. [14], respectively.

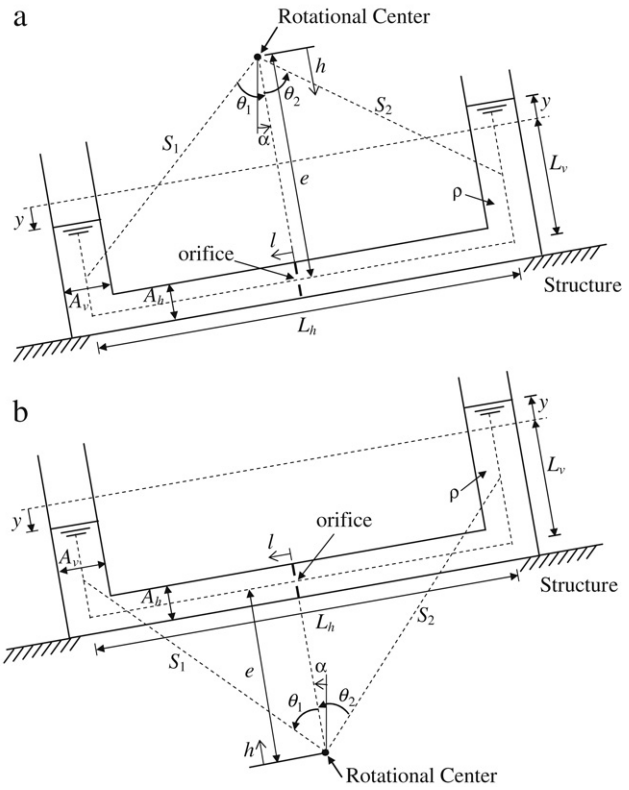

Fig. 1. Schematic diagram of a structure with a TLCD in pitching motion: (a) Horizontal column of a TLCD is located below the rotational center; (b) Horizontal column of a TLCD is located above the rotational center.

To further extend this concept to TLCDs with non-uniform cross-sections leading to more practical considerations in applying to the structural control of bridge pitching motion, this paper theoretically derived and re-examined the interaction of a single-degree-of-freedom structure equipped with a non-uniform TLCD. To account for the complexity of the liquid motion in the TLCD, the derivation is carried out by completely adopting the energy principle, the so-called Lagrange's equation approach, for the sake of avoiding the possibility of missing any terms. From the equations of motion derived, it was intriguingly found that there exists an additional term which was never revealed in existing relevant papers. A preliminary study through simulation further ascertained that the effect of the additional term is significant to the response, particularly when the TLCD horizontal length ratio becomes smaller and the ratio of the mass moment of inertia becomes larger.

The objective in the second part of this study was to experimentally verify the existence of this additional term. Large scale models of TLCDs and structures were constructed, and tests for identifying the individual parts as well as the interacted system subjected to harmonic loading were performed for verification. For comparison with the experimental results, a non-iterative analytical solution of such an interaction under harmonic loading was also derived to facilitate computation.

2. Interacted equations in pitching motion

The schematic diagram of a single-degree-of-freedom rotational structure (representing a bridge deck in the pitching motion) equipped with a TLCD under wind excitation is shown in Fig. 1(a) and (b). Each sketches the situation when the elevation of the horizontal column of a TLCD is below or above the rotational center of a deformed structure. In general, the cross-sections in horizontal and vertical columns of a TLCD can be non-uniform, depending

on the choice of the designer. Some presumptions for TLCDs were used herein to derive the equations of motion: (i) the fluid is incompressible (i.e., the flow rate is invariant), depicting that water is a good choice; (ii) the sloshing behavior on the liquid surface is negligible (this is reasonably satisfied if the structural frequency is as low as 0.5 Hz or even lower, which is quite common for bridges); (iii) the in-plane width of the TLCD vertical column cross-section should be much smaller than its horizontal length.

2.1. Derivation by energy principle

By means of energy principles, the equations of interacted motion can be derived as follows. During pitching motion, as shown in Fig. 1, the total kinetic energy T is the sum of those from the structure and TLCD as well, i.e.,

$$T = T_{\text{structure}} + T_{\text{TLCD}} \tag{1}$$

in which the kinetic energy of the structure, $T_{\text{structure}}$, is

$$T_{\text{structure}} = \frac{1}{2} J_\alpha \dot{\alpha}^2; \tag{2}$$

and the kinetic energy of the TLCD, T_{TLCD}, is composed of three parts, each part from different sections of the liquid column, i.e.,

$$T_{\text{TLCD}} = T_{\text{Left vertical column}} + T_{\text{Right vertical column}} + T_{\text{Horizontal column}} \tag{3}$$

with

$$\begin{aligned}
T_{\text{Left vertical column}} &= \frac{1}{2}\rho\,(L_v - y)\,A_v \left(\dot{y} + \frac{L_h}{2}\dot{\alpha}\right)^2 \\
&\quad \pm \frac{1}{2}\rho A_v \cdot \int_{e \mp L_v \pm y}^{e} (h\dot{\alpha})^2\,\mathrm{d}h \\
T_{\text{Right vertical column}} &= \frac{1}{2}\rho\,(L_v + y)\,A_v \left(\dot{y} + \frac{L_h}{2}\dot{\alpha}\right)^2 \\
&\quad \pm \frac{1}{2}\rho A_v \cdot \int_{e \mp L_v \mp y}^{e} (h\dot{\alpha})^2\,\mathrm{d}h \\
T_{\text{Horizontal column}} &= \frac{1}{2}\rho A_h L_h \left(\frac{A_v}{A_h}\dot{y} \pm e\dot{\alpha}\right)^2 \\
&\quad + \frac{1}{2}\rho A_h \cdot \int_{-L_h/2}^{L_h/2} (l\dot{\alpha})^2\,\mathrm{d}l.
\end{aligned} \tag{4}$$

In Eqs. (2) and (4), α and y denote the rotational angle of the structure and liquid displacement in the TLCD, respectively; J_α is the mass moment of inertia of the structure with respect to the rotational center; ρ is the fluid density; $A_h(A_v)$ and $L_h(L_v)$ are the cross-sectional area and column length of the horizontal (vertical) liquid columns; e is the vertical distance between the rotational center of the structure and the horizontal liquid column; and h and l are the integrating variables representing the position coordinates as indicated in Fig. 1. During the motion, the value of y should be kept within the difference of L_v and one half of the in-plane width of the horizontal column cross-section for maintaining consistent U-shape liquid movement. The upper and lower signs in symbols $\pm$ or $\mp$ are the operations corresponding to the situations in Fig. 1(a) and (b). Similarly, the potential energy in the system can be expressed as the sum of those from the structure and TLCD, i.e.,

$$V = V_{\text{structure}} + V_{\text{TLCD}} \tag{5}$$

in which the strain energy conserved in the structure, $V_{\text{structure}}$, is

$$V_{\text{structure}} = \frac{1}{2} K_\alpha \alpha^2; \tag{6}$$

and the potential energy of the liquid in the TLCD, V_{TLCD}, is composed of three parts, each part from different sections of the liquid column, i.e.,

$$V_{\text{TLCD}} = V_{\text{Left vertical column}} + V_{\text{Right vertical column}} + V_{\text{Horizontal column}} \tag{7}$$

with

$$\begin{aligned}
V_{\text{Left vertical column}} &= \mp \rho g A_v\,(L_v - y)\,[S_1 \cos(\theta_1 \mp \alpha)] \\
V_{\text{Right vertical column}} &= \mp \rho g A_v\,(L_v + y)\,[S_2 \cos(\theta_2 \pm \alpha)] \\
V_{\text{Horizontal column}} &= \mp \rho g A_h L_h e \cos\alpha.
\end{aligned} \tag{8}$$

In Eqs. (6) and (8), K_α is the rotational stiffness constant of the structure; g is acceleration due to gravity; $S_1(S_2)$ is the distance between the structural rotational center and the center of the left (right) vertical liquid column during the motion, and the corresponding angle formed with the TLCD center line is $\theta_1(\theta_2)$, as depicted in Fig. 1. Note that the point of zero potential energy is taken at the rotational center of the structure. After some arrangements, the kinetic energy T and potential energy V in Eqs. (1)–(8) can be simplified as

$$\begin{aligned}
T &= \frac{1}{2} J_\alpha \dot{\alpha}^2 + \rho A_v L_v \left(\dot{y} + \frac{L_h}{2}\dot{\alpha}\right)^2 \\
&\quad + \frac{1}{3}\rho A_v \dot{\alpha}^2 \left[3e^2 L_v \mp 3eL_v^2 + L_v^3 + 3y^2\,(\mp e + L_v)\right] \\
&\quad + \frac{1}{2}\rho A_h L_h \left(\frac{A_v}{A_h}\dot{y} \pm e\dot{\alpha}\right)^2 + \frac{1}{3}\rho A_h \dot{\alpha}^2 \left(\frac{L_h}{2}\right)^3
\end{aligned} \tag{9}$$

and

$$\begin{aligned}
V &= \frac{1}{2} K_\alpha \alpha^2 \mp \rho g A_h L_h e \cos\alpha \mp 2\rho g A_v L_v e \cos\alpha \\
&\quad + \rho g A_v (L_v^2 + y^2)\cos\alpha + \rho g A_v L_h y \sin\alpha
\end{aligned} \tag{10}$$

in which the relations $S_1 \cos\theta_1 = e \mp (L_v - y)/2$, $S_2 \cos\theta_2 = e \mp (L_v + y)/2$ and $S_1 \sin\theta_1 = S_2 \sin\theta_2 = L_h/2$ have been used for rearranging V. As observed in Eqs. (9) and (10), the sign $\pm$ (or $\mp$) appears simultaneously with the distance e. Thus, for conciseness in the expressions, the convention of e is defined to be positive or negative as the horizontal column of a TLCD is located below or above the rotational center of a structure, and this convention will be used throughout this paper in what follows.

From Newtonian mechanics, the energy principle — the Lagrange's equations expressed by

$$\begin{aligned}
\frac{\mathrm{d}}{\mathrm{d}t}\left(\frac{\partial\,(T - V)}{\partial \dot{\alpha}}\right) - \frac{\partial\,(T - V)}{\partial \alpha} &= Q_{nc,\alpha}; \\
\frac{\mathrm{d}}{\mathrm{d}t}\left(\frac{\partial\,(T - V)}{\partial \dot{y}}\right) - \frac{\partial\,(T - V)}{\partial y} &= Q_{nc,y}
\end{aligned} \tag{11}$$

shall represent the equations of the interacted motion, in which $Q_{nc,\alpha}$ and $Q_{nc,y}$ are the non-conservative forces in the directions of generalized coordinates α and y, respectively. In this study, $Q_{nc,\alpha}$ is the sum of the structural viscous damping moment expressed by $-C_\alpha \dot{\alpha}$, and the external moment $M(t)$ with respect to the rotational center. The term $Q_{nc,y}$, which is in fact the energy-dissipating force induced by the head loss of flow passing through the orifice in the horizontal column of the TLCD, is equal to $-\frac{1}{2}\rho\eta\left(\frac{A_v}{A_h}\right)\dot{y}\left|\left(\frac{A_v}{A_h}\right)\dot{y}\right| A_h$, in which η is the so-called head loss coefficient. With the assumption of $\alpha \ll 1$ (which implies $\sin\alpha \approx \alpha$ and $\cos\alpha \approx 1$), the resultant equations of motion for the structure and liquid surface displacement can be obtained as

$$\begin{aligned}
&(J_d + J_\alpha)\ddot{\alpha} + C_\alpha \dot{\alpha} + K_\alpha \alpha + \rho\nu A_h L_h\,(L_v + e)\,\ddot{y} \\
&\quad + \rho g A_h (L_h + 2\nu L_v) e\alpha + \rho g \nu A_h L_h y - \rho g \nu A_h L_v^2 \alpha = M(t)
\end{aligned} \tag{12}$$

and

$$\begin{aligned}
&\rho\nu A_h L_h\,(L_v + e)\,\ddot{\alpha} + \rho\nu A_h (2L_v + \nu L_h)\ddot{y} \\
&\quad + \frac{1}{2}\rho\eta\nu^2 A_h \dot{y}|\dot{y}| + \rho g \nu A_h L_h \alpha + 2\rho g \nu A_h y = 0
\end{aligned} \tag{13}$$

in which $\nu = A_v/A_h$ is the cross-section ratio of the vertical column versus horizontal column, $J_d = \rho A_h[(1/2)\nu L_v L_h^2 + 2\nu e^2 L_v - 2\nu e L_v^2 + (2/3)\nu L_v^3 + L_h e^2 + (1/12)L_h^3]$ is the mass moment of inertia of the fluid contained in a TLCD with respect to the rotational center. It is noted that all the terms involving the nonlinear terms of α and y, including three terms in the left hand side of Eq. (12), i.e., $-\rho g \nu A_h y^2 \alpha - 4\rho\nu A_h(e-L_v)y\dot{y}\dot{\alpha} - 2\rho\nu A_h(e-L_v)y^2\ddot{\alpha}$, and one term in the left hand side of Eq. (13), i.e., $2\rho\nu A_h(e-L_v)y\dot{\alpha}^2$, have been neglected under the assumption $\alpha \ll 1$ and $y/L_h \ll 1$. Their trivial contribution can be more easily observed if nondimensionalization is performed on them according to the procedure described in Section 2.2.

As observed from Eq. (12), the additional term $-\rho g \nu A_h L_v^2 \alpha$ which can be actually traced back to the potential energy $V_{\text{Left vertical column}} + V_{\text{Right vertical column}}$ is never considered in the existing literature (i.e., [12–14]). It will be denoted as the additional term in what follows in this paper. Since this additional term is a linear function of α, it will contribute an extra stiffness to the structure and therefore alter the natural frequency of the structure.

In the case that the structural motion is specified, the liquid motion in the TLCD can be determined by Eq. (13) only. As such, the natural frequency of a TLCD can be easily shown as $\omega_d = \sqrt{2g/L_e}$, in which $L_e = 2L_v + \nu L_h$ is defined as the effective length of liquid column. Consequently, the natural period of a TLCD, T_d, is equal to $2\pi\sqrt{L_e/2g}$. Note that the effective length L_e is equal to the total length L of the liquid column if all cross-sections are uniform (i.e., $\nu = 1$).

Since this paper conducted a basic research on the interaction between a structure and TLCD in pitching motion, a single-degree-of-freedom structure is used for simplicity. For a multiple-degree-of-freedom system with a dominant torsional mode in the higher mode, the torsional modal equation should be obtained by performing the modal decomposition technique with the torsional mode shape component at the location where the TLCD is installed set to one. Then the corresponding modal mass, stiffness and damping will be used as the structural properties in the formula described above.

2.2. Nondimensionalization for equations of motion

To facilitate further derivation, nondimensionalization for the equations of motion in Eqs. (12) and (13) was performed and the resultant equations are expressed as

$$(1+\mu)\alpha'' + 4\pi\xi\beta_1\alpha' + 4\pi^2\beta_1^2\alpha + \frac{\nu\varepsilon r}{p}\hat{y}'' + 2\pi^2\frac{\nu\varepsilon q}{mn}\alpha + 2\pi^2\frac{\nu\varepsilon}{n}\hat{y} - \frac{\pi^2\nu\varepsilon}{2n}\left(\frac{1}{p}-1\right)^2\alpha = \hat{M}(\hat{t}) \tag{14}$$

$$\frac{nr}{p}\alpha'' + \hat{y}'' + \frac{1}{2}\nu n\eta\,|\hat{y}'|\,\hat{y}' + 2\pi^2\alpha + 4\pi^2\hat{y} = 0 \tag{15}$$

in which $(')$ represents the differentiation with respect to $\hat{t} = t/T_d$. Other nondimensional quantities are defined as follows: $\hat{y} = y/L_h$; $\hat{M}(\hat{t}) = MT_d^2/J_\alpha$; $\beta_1 = \omega_\alpha/\omega_d$ is the natural frequency ratio of the structure versus TLCD ($\omega_\alpha = \sqrt{K_\alpha/J_\alpha}$ is the structural natural frequency); $\xi = C_\alpha/2J_\alpha\omega_\alpha$ is the structural damping ratio; $p = L_h/L$ is the ratio of the horizontal column length versus total length of a TLCD; $q = e/L_h$ is the ratio of the distance between the rotational center and horizontal column versus the TLCD horizontal column length; m and n are two parameters related to p and ν (i.e., $m = \nu p/(\nu + p(1-\nu))$ is the ratio of νL_h versus $(L_h + 2\nu L_v)$ and $n = p/(1-p(1-\nu))$ is the ratio of L_h versus L_e); r is a parameter depending on p and q (i.e., $r = pq + (1-p)/2$); $\mu = J_d/J_\alpha$ is the ratio of mass moment of inertia of the TLCD versus structure; and $\varepsilon = \rho A_h L_h^3/J_\alpha$. The parameters μ and ε are related to each other by

$$\mu = \varepsilon\left[\frac{1}{2}\nu\left(\frac{1-p}{2p}\right) + 2\nu q^2\left(\frac{1-p}{2p}\right) - 2\nu q\left(\frac{1-p}{2p}\right)^2 + \frac{2}{3}\nu\left(\frac{1-p}{2p}\right)^3 + q^2 + \frac{1}{12}\right],$$

which can be obtained by expressing J_d as a function of ε, p, q and ν. It is noticed that the term $-\frac{\pi^2\nu\varepsilon}{2n}\left(\frac{1}{p}-1\right)^2\alpha$ in Eq. (14) is the additional term in the dimensionless form.

2.3. Equivalent viscous damping under harmonic loading

If a system is subjected to a harmonic type of loading, the nonlinear damping force term $(1/2)\rho\eta\nu^2 A_h\dot{y}|\dot{y}|$ in Eq. (13) can be replaced by an equivalent viscous damping force expressed as $\frac{4}{3\pi}\rho\eta\nu^2 A_h\varphi_y\omega\dot{y}$, in which φ_y is the amplitude of liquid displacement y and ω is the circular excitation frequency (see Gao et al. [5]). This relationship can be easily derived by equating the energy dissipated in one cycle by the nonlinear damping force and that by the equivalent viscous damping force. Thus, the nondimensionalized equation in Eq. (15) can be rewritten as

$$\frac{nr}{p}\alpha'' + \hat{y}'' + \frac{8}{3}\nu n\eta\varphi_{\hat{y}}k\hat{y}' + 2\pi^2\alpha + 4\pi^2\hat{y} = 0 \tag{16}$$

in which $k = \omega/\omega_d$ is the ratio of the excitation frequency versus TLCD natural frequency (excitation frequency ratio); and $\varphi_{\hat{y}} = \varphi_y/L_h$ is the nondimensionalized amplitude of the liquid displacement.

2.4. Analytical solution to harmonic loading

By replacing α, $\hat{y}$ and $\hat{M}(\hat{t})$ by the complex harmonic functions $\alpha_0 e^{i2\pi k\hat{t}}$, $\hat{y}_0 e^{i2\pi k\hat{t}}$ and $\hat{M}_0 e^{i2\pi k\hat{t}}$ ($i = \sqrt{-1}$), respectively, the complex amplitude α_0 and $\hat{y}_0$ can be obtained as functions of the force amplitude $\hat{M}_0$, i.e.,

$$\alpha_0 = T_{\alpha\hat{M}}\hat{M}_0 \tag{17}$$

$$\hat{y}_0 = T_{\hat{y}\hat{M}}\hat{M}_0 \tag{18}$$

in which $T_{\alpha\hat{M}}$ and $T_{\hat{y}\hat{M}}$ are the frequency response functions of α and $\hat{y}$ induced by $\hat{M}$, expressed as

$$T_{\alpha\hat{M}} = \frac{2\left(1-k^2\right) + i\left(\frac{8}{3\pi}k^2\nu n\eta\varphi_{\hat{y}}\right)}{G}; \qquad T_{\hat{y}\hat{M}} = \frac{\left(2k^2\frac{nr}{p}-1\right)}{G} \tag{19}$$

with

$$G = (T_B + T_C\cdot\varphi_{\hat{y}}) + i(T_D + T_E\cdot\varphi_{\hat{y}}) \tag{20}$$

$$T_B = 8\pi^2\left(1-k^2\right)\left[\beta_1^2 - k^2(1+\mu) + \frac{\nu\varepsilon q}{2mn} - \frac{\nu\varepsilon}{8n}\left(\frac{1}{p}-1\right)^2\right] - 2\pi^2\varepsilon\left(\frac{\nu}{n} - 4k^2\frac{\nu r}{p} + 4k^4\frac{\nu n r^2}{p^2}\right)$$

$$T_C = -\frac{64}{3}\pi k^3\nu n\eta\xi\beta_1; \qquad T_D = 16\pi^2 k\xi\beta_1\left(1-k^2\right) \tag{21}$$

$$T_E = \frac{32}{3}\pi k^2\nu n\eta\left[\left(\beta_1^2 + \frac{\nu\varepsilon q}{2mn}\right) - k^2(1+\mu) - \frac{\nu\varepsilon}{8n}\left(\frac{1}{p}-1\right)^2\right].$$

By using the relation $\varphi_{\hat{y}} = |\hat{y}_0|$, the substitution of Eqs. (19)–(21) into square of the absolute value on both sides of Eqs. (17) and (18) leads to

$$|\alpha_0|^2 = \frac{T_F \cdot \hat{M}_0^2}{\left(T_B + T_C \cdot |\hat{y}_0|\right)^2 + \left(T_D + T_E \cdot |\hat{y}_0|\right)^2} \tag{22}$$

$$|\hat{y}_0|^2 = \frac{T_A \cdot \hat{M}_0^2}{\left(T_B + T_C \cdot |\hat{y}_0|\right)^2 + \left(T_D + T_E \cdot |\hat{y}_0|\right)^2} \tag{23}$$

in which

$$T_F = 4(1-k^2)^2 + \left(\frac{8}{3\pi}k^2 \nu n \eta\, |\hat{y}_0|\right)^2; \qquad T_A = \left(2k^2\frac{nr}{p} - 1\right)^2. \tag{24}$$

By further rearranging Eq. (23) into a polynomial in $|\hat{y}_0|$ expressed as

$$C_4 |\hat{y}_0|^4 + C_3 |\hat{y}_0|^3 + C_2 |\hat{y}_0|^2 + C_0 = 0 \tag{25}$$

in which

$$C_4 = T_C^2 + T_E^2; \quad C_3 = 2(T_B \cdot T_C + T_D \cdot T_E); \quad C_2 = T_B^2 + T_D^2; \quad C_0 = -T_A \cdot \hat{M}_0^2, \tag{26}$$

the value of $|\hat{y}_0|$ can be solved analytically. It can be shown by extensive simulation from Eq. (25) that $|\hat{y}_0|$ has an unique positive or zero solution. Consequently, the frequency response function $T_{\alpha\hat{M}}$, $T_{\hat{y}\hat{M}}$ and the amplitude $|\alpha_0|$ can be obtained by substituting the solution of $|\hat{y}_0|$ back into Eqs. (19) and (22), respectively. It should be noticed that the system is in fact not linear because both of the frequency response functions $T_{\alpha\hat{M}}$ and $T_{\hat{y}\hat{M}}$ depend on the value of $\hat{M}_0$. To calculate the responses without the additional term considered, the same formula and procedures will apply except that the term $-\nu\varepsilon((1/p) - 1)^2/(8n)$ involved in T_B and T_E of Eq. (21) should be dropped.

To clarify the significance of difference caused by the additional term, extensive simulated results of the analytical responses under harmonic loading were calculated, using the equations provided in Eqs. (22), (23) and (25), and the comparison between those with and without the additional term included was made in the preliminary study. It is obvious that the significance of the difference in $|\alpha_0|$ and $|\hat{y}_0|$ caused by the additional term depends on the parameters (μ, p, k and others) that are chosen. Some typical results were tabulated in Table 1 with the parameter μ varying from 2% to 10%, ν from 1 to 3 and p from 0.5 to 0.7. This table contains the responses $|\alpha_0|$ and $|\hat{y}_0|$ at the frequency ratio k where the largest discrepancy occurs (largest relative error). The common parameters used for generating the results in Table 1(a) and (b) are $\hat{M}_0 = 0.7$, $\xi = 1\%$, $\beta_1 = 1$ and $\eta = 5$. The parameter $\beta_1$is taken herein as 1.0 in that the TLCD frequency is always tuned to the vicinity around the structural frequency in the optimal design (see [8,12–14]). The difference in the parameters of Table 1(a) and (b) is the value of q, which is taken to be 0.1 in (a) and 0.4 in (b) for scrutinizing the effect of the TLCD location with respect to the structure.

As shown in Table 1, the effect of the additional term is more significant when p becomes smaller and μ becomes larger in general. In some particular cases as shown in Table 1(b), for instance, when p is equal to 0.5, a mere 2% of μ can result in $|\alpha_0|$ relative error as large as 29.59% for $\nu = 2$. To illustrate the variation of difference caused by the additional term versus the variation of the excitation frequency ratio k, the plots of responses were shown in Fig. 2(a) and (b) for the two cases with the biggest relative errors in Table 1(a) and (b) (Case 1: $q = 0.1$, $p = 0.5$, $\nu = 3$, $\mu = 10\%$; (b) Case 2: $q = 0.4$, $p = 0.5$, $\nu = 1$, $\mu = 10\%$). As shown in Fig. 2, the responses caused by the additional term are obviously different because the term provides an additional stiffness to the original structure, and the difference in $|\alpha_0|$ and $|\hat{y}_0|$ varies with the excitation frequency ratio k.

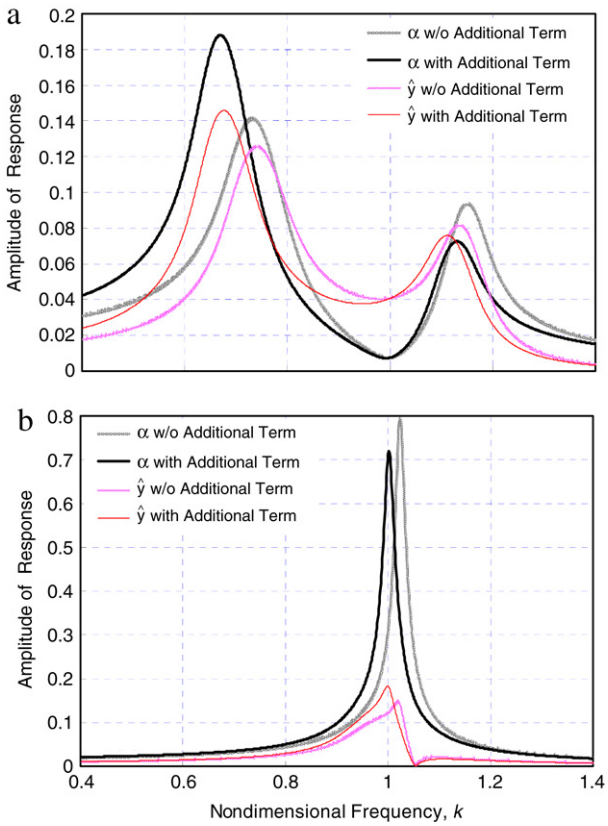

Fig. 2. Comparisons of the simulated analytical responses versus k under harmonic loading; (a) Case 1: $\hat{M}_0 = 0.7$, $\xi = 1\%$, $\beta_1 = 1$, $\eta = 5$, $q = 0.1$, $p = 0.5$, $\nu = 3$, $\mu = 10\%$; (b) Case 2: $\hat{M}_0 = 0.7$, $\xi = 1\%$, $\beta_1 = 1$, $\eta = 5$, $q = 0.4$, $p = 0.5$, $\nu = 1$, $\mu = 10\%$.

In the practical application to bridges, using a 2% value of μ is reasonable (normally 1%–3%). A value of 0.5 or 0.6 for p is possible if the bridge deck (most possibly box girder) inside has no enough horizontal space for the TLCD. For example, if a uniform TLCD is tuned to 0.15 Hz, the required total column length L is 22.11 m. Thus, the horizontal length calculated by using $p = 0.5$–0.6 is 11.05–13.27 m, which is a space-demanding requirement. A larger p will even result in a bigger demand in horizontal space, which is not possible to be achieved in actual implementation.

Therefore, in order to verify the existence of this additional term, large scale models for TLCDs and structure were constructed and extensive tests for identifying the individual parts as well as the interacted system subjected to harmonic loading were performed. The pertinent experimental results, including the setup and procedures, will be described in the next three Sections 3–5.

3. Tests for identifying structural properties

To model the pitching motion of bridge sections, a large scale spring-constrained steel beam pivoted at mid-span, which represents a typical single-degree-of-freedom rotational structure, was constructed in the structural laboratory of National Chiao Tung University, Taiwan. The configuration and picture of the experimental setup were shown in Fig. 3(a) and (b), respectively. Since the TLCD frame (without fluid) contains mass, it should be included as one part of the structural mass. To magnify the interaction effect

Table 1
Comparisons of the simulated analytical responses under harmonic loading:

			$\lvert\alpha_0\rvert$				$\lvert y_0\rvert$			
p	ν	μ (%)	k	Without additional term	With additional term	Relative error (%)	k	Without additional term	With additional term	Relative error (%)
(1)	(2)	(3)	(4)	(5)	(6)	(7)	(8)	(9)	(10)	(11)
(a) $\hat{M}_0 = 0.7, \xi = 1\%, \beta_1 = 1, \eta = 5, q = 0.1$										
0.5	1	2	0.977	0.3572	0.4343	21.58	0.977	0.2727	0.3010	10.39
		3	0.969	0.2803	0.3487	24.38	1.006	0.2566	0.2259	−12.00
		5	1.006	0.2439	0.1833	−24.86	0.865	0.1054	0.1232	16.96
		10	0.826	0.1033	0.1478	43.07	0.821	0.0884	0.1241	40.37
	2	2	1.018	0.2264	0.1890	−16.50	0.849	0.1002	0.1092	9.02
		3	0.847	0.0946	0.1099	16.10	0.830	0.0932	0.1066	14.34
		5	0.803	0.0882	0.1135	28.62	0.797	0.0842	0.1069	26.89
		10	0.722	0.0836	0.1453	73.79	0.720	0.0673	0.1158	72.00
	3	2	0.836	0.0877	0.0998	13.78	0.819	0.0907	0.1018	12.31
		3	0.801	0.0830	0.1008	21.52	0.793	0.0834	0.1002	20.06
		5	0.751	0.0816	0.1150	41.00	0.748	0.0744	0.1038	39.48
		10	0.640	0.0756	0.1668	120.63	0.639	0.0555	0.1216	119.05
0.6	1	2	1.010	0.3539	0.3222	−8.96	1.010	0.2527	0.2411	−4.59
		3	1.012	0.2667	0.2399	−10.04	1.012	0.2182	0.2070	−5.17
		5	1.023	0.1653	0.1487	−10.04	0.842	0.0970	0.1046	7.79
		10	0.797	0.0998	0.1183	18.60	0.793	0.0859	0.1012	17.78
	2	2	1.043	0.1425	0.1332	−6.54	0.824	0.0921	0.0967	5.08
		3	0.810	0.0866	0.0941	8.66	0.801	0.0870	0.0940	8.06
		5	0.764	0.0877	0.1013	15.58	0.760	0.0804	0.0925	14.99
		10	0.669	0.0927	0.1296	39.83	0.668	0.0706	0.0984	39.28
	3	2	0.797	0.0821	0.0888	8.10	0.789	0.0852	0.0917	7.57
		3	0.761	0.0834	0.0941	12.89	0.757	0.0805	0.0904	12.36
		5	0.700	0.0872	0.1089	24.85	0.699	0.0743	0.0923	24.33
		10	0.564	0.0939	0.1644	75.02	0.564	0.0636	0.1110	74.54
0.7	1	2	1.014	0.2841	0.2739	−3.58	1.014	0.2253	0.2212	−1.81
		3	1.020	0.2010	0.1935	−3.74	0.846	0.0976	0.0994	1.91
		5	0.831	0.0956	0.0991	3.64	0.820	0.0911	0.0941	3.35
		10	0.768	0.0971	0.1047	7.80	0.765	0.0835	0.0898	7.54
	2	2	0.811	0.0840	0.0864	2.86	0.800	0.0872	0.0895	2.64
		3	0.777	0.0845	0.0883	4.42	0.772	0.0834	0.0869	4.20
		5	0.724	0.0903	0.0976	8.07	0.721	0.0786	0.0847	7.87
		10	0.609	0.1053	0.1274	20.98	0.609	0.0754	0.0911	20.81
	3	2	0.761	0.0823	0.0860	4.51	0.756	0.0812	0.0848	4.31
		3	0.718	0.0871	0.0935	7.31	0.715	0.0780	0.0836	7.12
		5	0.642	0.0974	0.1115	14.44	0.641	0.0754	0.0862	14.27
		10	0.464	0.1246	0.1837	47.43	0.464	0.0762	0.1123	47.30
(b) $\hat{M}_0 = 0.7, \xi = 1\%, \beta_1 = 1, \eta = 5, q = 0.4$										
0.5	1	2	0.992	0.5292	0.6604	24.80	0.992	0.1699	0.1899	11.76
		3	0.993	0.4885	0.6737	37.92	0.993	0.1618	0.1901	17.49
		5	0.995	0.4227	0.6967	64.81	0.995	0.1479	0.1900	28.43
		10	0.997	0.2859	0.6602	130.91	0.997	0.1195	0.1816	52.01
	2	2	0.992	0.3196	0.4141	29.59	0.992	0.2167	0.2467	13.86
		3	0.992	0.2413	0.3243	34.40	0.992	0.1882	0.2183	15.96
		5	0.994	0.1575	0.2109	33.89	1.097	0.0754	0.0610	−19.07
		10	1.096	0.2046	0.1165	−43.04	0.830	0.0605	0.0837	38.31
	3	2	0.987	0.1804	0.2201	22.00	1.042	0.1862	0.1657	−11.02
		3	1.065	0.1859	0.1467	−21.07	0.836	0.0763	0.0877	14.92
		5	0.821	0.0698	0.0892	27.84	0.813	0.0672	0.0847	26.11
		10	0.769	0.0604	0.0750	61.44	0.766	0.0523	0.0836	59.66
0.6	1	2	0.991	0.5688	0.6269	10.21	0.991	0.1754	0.1842	5.00
		3	0.991	0.5292	0.6095	15.18	0.991	0.1692	0.1816	7.35
		5	0.992	0.4834	0.6035	24.84	0.992	0.1605	0.1794	11.77
		10	0.994	0.3898	0.5716	46.66	0.994	0.1420	0.1721	21.14
	2	2	0.990	0.3039	0.3402	11.97	1.024	0.2111	0.1987	−5.86
		3	0.989	0.2233	0.2518	12.81	1.033	0.1821	0.1698	−6.76
		5	1.056	0.1991	0.1712	−14.02	1.110	0.0638	0.0582	−8.89
		10	1.112	0.1392	0.1103	−20.82	1.126	0.0586	0.0481	−17.82
	3	2	1.049	0.1863	0.1700	−8.75	0.835	0.0816	0.0855	4.88
		3	1.089	0.1368	0.1240	−9.34	0.818	0.0760	0.0817	7.46
		5	1.143	0.1045	0.0902	−13.66	0.789	0.0685	0.0774	12.99
		10	0.734	0.0701	0.0910	29.83	0.732	0.0581	0.0750	29.24

Table 1 (*continued*)

			$\lvert\alpha_0\rvert$				$\lvert y_0\rvert$			
p	ν	μ (%)	k	Without additional term	With additional term	Relative error (%)	k	Without additional term	With additional term	Relative error (%)
(1)	(2)	(3)	(4)	(5)	(6)	(7)	(8)	(9)	(10)	(11)
0.7	1	2	0.990	0.5873	0.6111	4.06	0.990	0.1777	0.1813	2.02
		3	0.990	0.5668	0.6005	5.94	0.990	0.1746	0.1797	2.94
		5	0.990	0.5289	0.5786	9.39	0.989	0.1659	0.1736	4.60
		10	0.989	0.4313	0.5014	16.26	1.012	0.1436	0.1320	−8.05
	2	2	1.025	0.3024	0.2881	−4.72	1.026	0.1929	0.1883	−2.41
		3	1.036	0.2263	0.2147	−5.10	1.038	0.1607	0.1564	−2.66
		5	1.069	0.1549	0.1464	−5.49	1.122	0.0571	0.0549	−3.87
		10	1.129	0.1084	0.0986	−9.03	1.139	0.0509	0.0469	−7.88
	3	2	1.066	0.1432	0.1383	−3.40	0.819	0.0796	0.0815	2.36
		3	1.127	0.1003	0.0962	−4.06	0.798	0.0748	0.0775	3.63
		5	0.766	0.0760	0.0810	6.60	0.762	0.0687	0.0731	6.37
		10	0.691	0.0793	0.0910	14.71	0.690	0.0620	0.0710	14.51

Table 2
Identified results of the structure

Structure model (1)	Natural frequency ω_α (rad/s) (2)	Damping ratio ξ (%) (3)	Mass moment of inertia J_α (Nms^2) (4)
Beam + TLCD ($\nu = 2$) frame	$0.3623 \times 2\pi$	0.424	757.28
Beam + TLCD ($\nu = 3$) frame	$0.3010 \times 2\pi$	0.446	1015.94

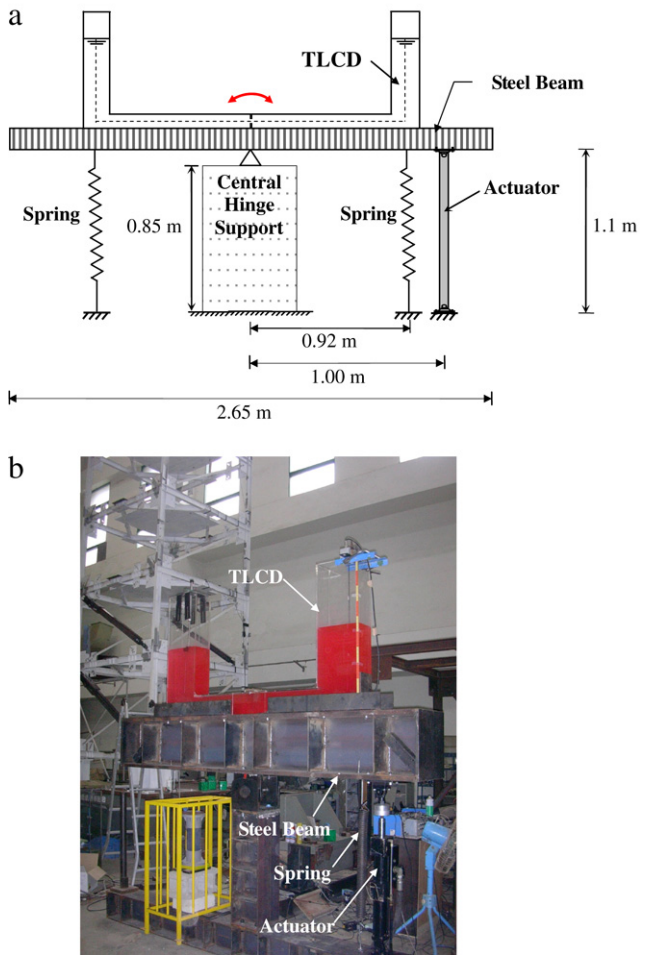

Fig. 3. Experimental setup of the spring-constrained steel beam and TLCD: (a) Configuration of the setup; (b) Picture of the setup.

between the TLCD and structure as needed for the interaction tests, their natural frequencies were principally designed to be kept close to each other. In the following tests, two sets of TLCD models were designed, denoted as $\nu = 2$ and $\nu = 3$ (see Section 4 for their detailed configurations), and the combined structural mass moments of inertia were accordingly adjusted by adding steel bricks on the steel beam so that the natural frequencies can comply with what were designed. Free vibration tests were performed by giving an initial rotation angle to the steel beam, and the responses were recorded. A direct measurement of peak-to-peak duration easily leads to the natural frequency ω_α, while the damping ratio ξ was obtained by using logarithmic decrement method. Additionally, the structural rotational stiffness K_α can be identified from the moment-rotation relation that was performed using the driving actuator shown in Fig. 3. Based on the relation $K_\alpha = J_\alpha \omega_\alpha^2$, the mass moment of inertia J_α can be thus computed. The identified results of the structure were tabulated in Table 2.

4. Tests for identifying TLCD properties

Two sets of TLCD models with horizontal length ratio ν equal to 2 and 3 were designed for the tests. Their detailed configurations were listed in Table 3, in which the values of theoretical natural frequencies provided in Eq. (13) are also shown for comparison with test results. In the mid-span of the TLCD horizontal column, five sets of orifice plates with blocking ratio ψ ranging from 0% (fully open), 20%, 40%, 60% to 80% were designed to provide different choices of energy-dissipating capabilities that corresponds to different head loss coefficients to be identified. To identify the TLCD properties such as the natural frequency and head loss, the TLCDs were placed on the top of the steel beam which can be driven by an actuator as a platform for generating rotational motion (see Fig. 3).

4.1. TLCD natural frequency

The natural frequencies of TLCDs were identified by free vibration tests. With the actuator commanded in displacement mode, a harmonic rotation is firstly specified to the steel beam for a certain duration of time until an appreciable liquid motion is formed. A sudden stop of the actuator at the equilibrium (horizontal) position can lead to a simple free vibration of the liquid surface. In this way, the TLCD natural frequency ω_d can be directly measured from the peak-to-peak duration of the wave sensor readings. The case with a blocking ratio equal to 0% was used to minimize the damping effect. The identified frequencies of the two sets of TLCDs were shown in Table 4. Comparison with theoretical values shows that the relative errors are both less than 5%, which is fairly acceptable.

Table 3
Configurations of TLCD models

Configuration (1)	TLCD ($\nu = 2$) (2)	TLCD ($\nu = 3$) (3)
A_v (cm^2)	30 × 15	45 × 15
A_h (cm^2)	15 × 15	15 × 15
L_h (cm)	145	145
L_v (cm)	48.33	48.33
e (cm)	−62.5	−62.5
$\nu = A_v/A_h$	2	3
$L = L_h + 2L_v$ (cm)	241.66	241.66
$L_e = \nu L_h + 2L_v$ (cm)	386.66	531.66
J_d (Ns^{2}m)	74.671	102.807
$\mu = J_d/J_\alpha$ (%)	9.86	10.12
$p = L_h/L$	0.6	0.6
$q = e/L_h$	−0.43	−0.43
Theoretical natural frequency $\omega_d = (2g/L_e)^{1/2}$ (rad/s)	0.36 × 2π	0.31 × 2π
Blocking ratio ψ (%)	0, 20, 40, 60, 80	0, 20, 40, 60, 80

Table 4
Identified natural frequencies of TLCD models

TLCD model (1)	Identified natural frequency (rad/s) (2)	Relative error (%) (3)
TLCD ($\nu = 2$)	0.3722 × 2π	3.27
TLCD ($\nu = 3$)	0.3251 × 2π	4.64

Table 5
Identified head loss coefficients of TLCD models

Blocking ratio ψ (%) (1)	Head loss coefficient η	
	TLCD ($\nu = 2$) (2)	TLCD ($\nu = 3$) (3)
0	7.0	9.7
20	9.1	12.4
40	14.1	20.9
60	33.5	49.0
80	149.0	230.0

4.2. TLCD head loss coefficients

The head loss coefficients corresponding to various blocking ratios can be identified through a series of forced vibration tests, in which harmonic rotations with a fixed amplitude and a set of certain frequencies were specified to the steel beam by commanding the actuator in displacement mode. Theoretically, the analytical solution for the liquid displacement $\hat{y}$ under a harmonic rotation α of the structure can be derived in the following manner. By replacing α and $\hat{y}$ in Eq. (16) by $\alpha_0 e^{i2\pi k\hat{t}}$ and $\hat{y}_0 e^{i2\pi k\hat{t}}$, and according to $\varphi_{\hat{y}} = |\hat{y}_0|$, the steady-state amplitude of liquid displacement $\varphi_{\hat{y}}$ can be solved in terms of the rotation amplitude α_0, see Box I. In the tests, for each blocking ratio ψ, the harmonic motions with a fixed displacement amplitude of 30 mm (i.e., $\alpha_0 =$ 0.03 rad) and a series of different excitation frequencies were sequentially specified to the steel beam by commanding the actuator, and the steady-state response of the liquid displacement was correspondingly measured by the wave sensor. The relation of these liquid displacement amplitudes $|\hat{y}_0|$ versus the excitation frequencies ratio k ($k = \omega/\omega_d$) can be plotted and compared with analytical curve shown in Box I. By curve-fitting both curves, the value of the head loss coefficient η in Box I can be determined. Shown in Fig. 4(a) and (b) were the plots of $|\hat{y}_0|$ versus k for the two sets of TLCDs, respectively, where the experimental and curve-fitted responses are denoted by the marks and solid curves, respectively. The results of the identified head loss coefficients corresponding to different blocking ratios for the two sets of TLCD models were shown in Table 5. As observed from Table 5, the head loss coefficients increase monotonically with the blocking ratio ψ, and also with the cross-section ratio ν.

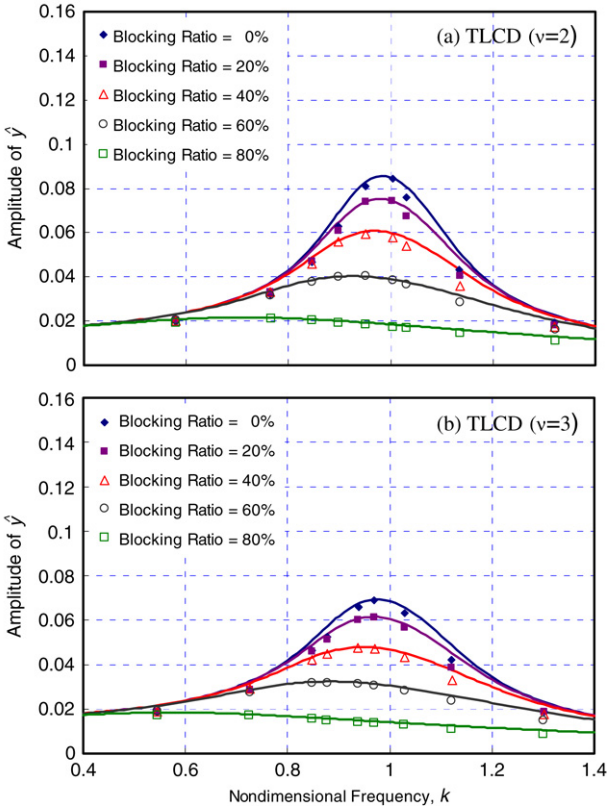

Fig. 4. Plots of $|\hat{y}_0|$ versus k (to identify head loss coefficients of TLCDs) : (a) TLCD ($\nu = 2$); (b) TLCD ($\nu = 3$).

5. Tests for interaction between TLCD and structure

Based on the analytical simulated results in Table 1 and Fig. 2, this section is to perform interaction tests on a structural model equipped with a TLCD to verify the existence of the additional term. Since this verification is focused on one term only, the best and most efficient way is to choose appropriate values of parameters (such as a larger μ and smaller p) such that the difference in the response caused by the additional term is as clear as possible. By the TLCD configurations shown in Table 3, the computed mass moments of inertia for the two sets of TLCDs are 74.670 and 102.807 Nms^2, which are corresponding to the ratios of mass moment of inertia ($\mu = J_d/J_\alpha$) equal to 9.86% and 10.12%, respectively. The horizontal length ratio p for both TLCDs ($\nu = 2$ and $\nu = 3$) is 0.6.

In this part of tests, the TLCD was placed on the top of the steel beam (see Fig. 3) so that a two-degree-of-freedom system is

$$\varphi_{\hat{y}} = |\hat{y}_0| = \frac{\sqrt{-2\pi^2(1-k^2)^2 + \left[4\pi^4(1-k^2)^4 + \left(\frac{8}{3}\nu n\eta k^2\right)^2 \pi^2 \left(2k^2 \frac{nr}{p} - 1\right)^2 \alpha_0^2\right]^{1/2}}}{\frac{8}{3}\nu n\eta k^2}$$

Box I.

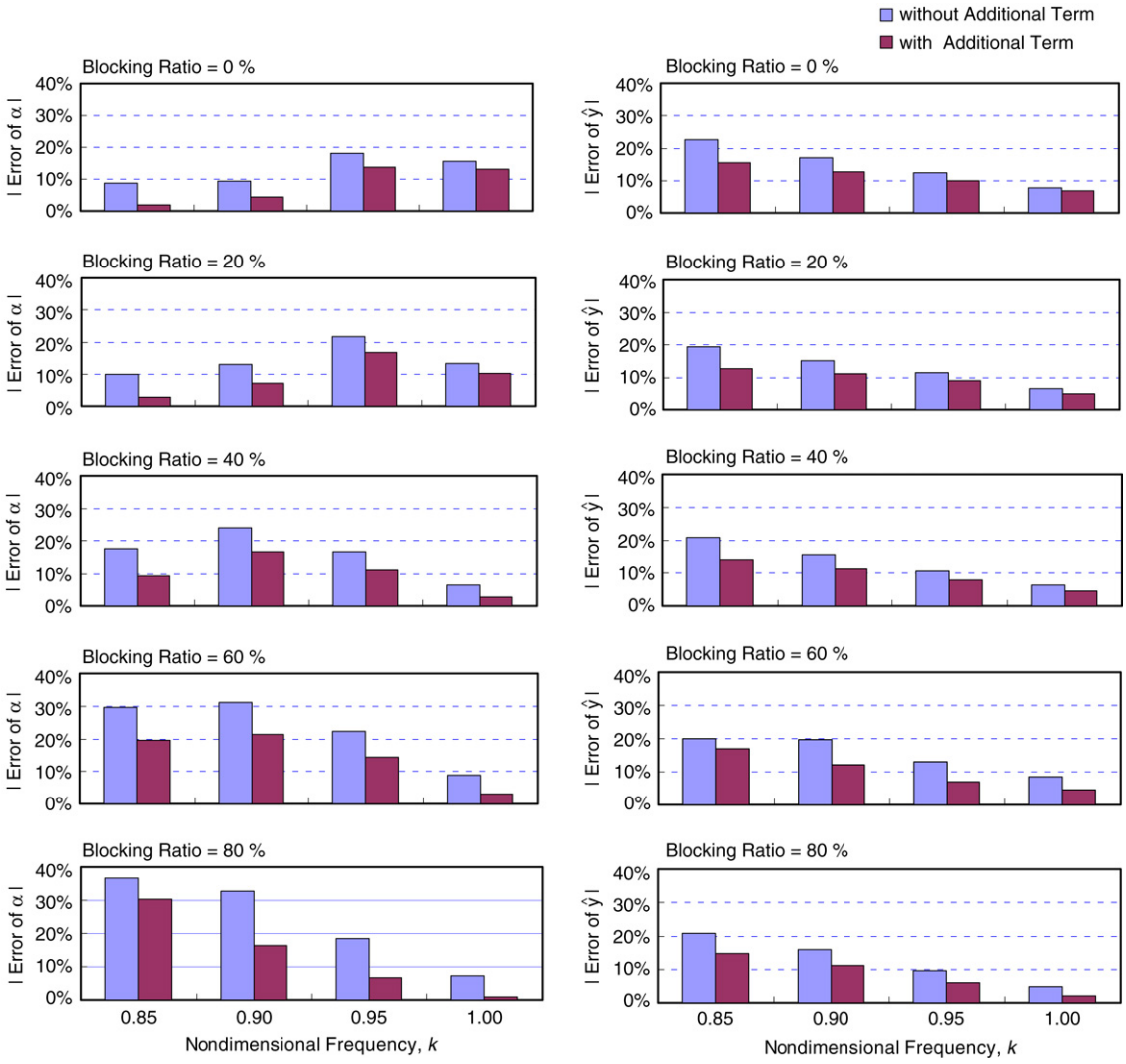

Fig. 5. Error comparison of the interacted responses w/wo the additional term considered for the test structure equipped with TLCD ($\nu = 2$).

formed to verify the interaction between the TLCD and structure. For each blocking ratio ψ, a series of forced vibration tests were performed by commanding the actuator in the displacement mode to provide a harmonic motion with a fixed amplitude of 30 mm (i.e., $\alpha_0 = 0.03$ rad) and a series of different frequencies to the steel beam. The use of displacement mode in 30 mm maximum is due to the limited capacity of the actuator to be operated within a sustainable stability. The steady-state external force applied to the steel beam (and moment M accordingly) was therefore measured by the load cell sensor installed between the actuator and the steel beam, whereas the steady-state responses including the liquid displacement of the TLCD and the rotation of the steel beam were measured by the wave and displacement sensors.

As mentioned in the Section 3, the natural frequency of the TLCD was designed to tune to that of the structure for magnifying the interaction effect. As a consequence of such a resonance effect, the structural response is reduced, while the liquid motion in the TLCD is amplified. Due to the fact that the interacted responses are sensitive to the external force which is not quite so easy to be accurately measured by the load cell under the interference of noise, to maximize experimental accuracy, the excitation frequencies in our interest for verifying the interaction effect are best represented by the ones near resonance, i.e., by choosing k near 1.

The interacted responses from tests for the two sets of TLCDs were tabulated in columns (4), (5) of Tables 6 and 7, respectively, in different conditions of blocking ratio. The simulated analytical responses without the additional term considered and with the additional term considered were also shown in columns (6), (7) and (8), (9), respectively, for comparison. In columns (6)–(9), the values inside the parentheses are the relative errors with respect to the experimental results shown in columns (4) and (5). The relative errors of the simulated responses in different conditions of blocking ratios for the two sets of TLCDs were also plotted in Figs. 5 and 6 for a better illustration. As observed from Tables 6 and 7 and Figs. 5 and 6, it is apparent that relative errors in

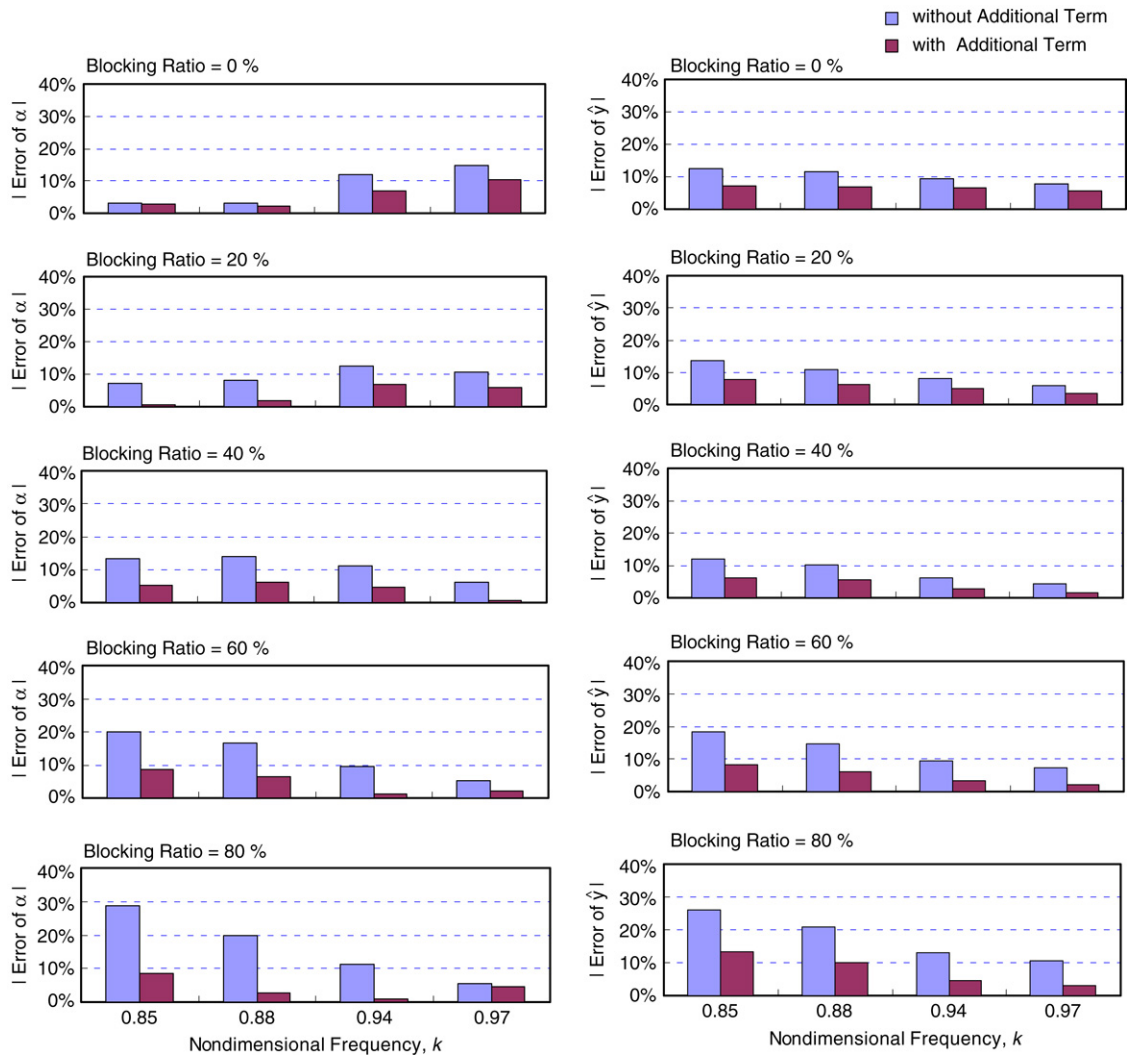

Fig. 6. Error comparison of the interacted responses w/wo the additional term considered for the test structure equipped with TLCD ($\nu = 3$).

Table 6
Comparison of experimental and analytical results in the pitching interaction of the structure and TLCD ($\nu = 2$)

Structure + TLCD ($\nu = 2$)								
			Experimental		Analytical			
					Without additional term		With additional term	
ψ (%) (1)	k (2)	$\hat{M}_0$ (3)	$\lvert\alpha_0\rvert$ (4)	$\lvert\hat{y}_0\rvert$ (5)	$\lvert\alpha_0\rvert$ (6)	$\lvert\hat{y}_0\rvert$ (7)	$\lvert\alpha_0\rvert$ (8)	$\lvert\hat{y}_0\rvert$ (9)
0	0.8458	0.529	0.03	0.04682	0.03261 (**8.70%**)	0.05737 (**22.53%**)	0.03057 (**1.90%**)	0.05407 (**15.48%**)
	0.8967	0.810	0.03	0.06297	0.03286 (**9.52%**)	0.07361 (**16.90%**)	0.03136 (**4.52%**)	0.07103 (**12.79%**)
	0.9500	1.062	0.03	0.08101	0.03543 (**18.10%**)	0.09102 (**12.35%**)	0.03413 (**13.75%**)	0.08912 (**10.00%**)
	1.0035	1.006	0.03	0.08440	0.03470 (**15.66%**)	0.09106 (**7.90%**)	0.03393 (**13.09%**)	0.09004 (**6.69%**)
20	0.8458	0.521	0.03	0.04722	0.03301 (**10.04%**)	0.05643 (**19.51%**)	0.03088 (**2.92%**)	0.05321 (**12.69%**)
	0.8969	0.775	0.03	0.06104	0.03386 (**12.87%**)	0.07026 (**15.11%**)	0.03219 (**7.29%**)	0.06777 (**11.02%**)
	0.9500	0.968	0.03	0.07392	0.03650 (**21.67%**)	0.08231 (**11.34%**)	0.03502 (**16.74%**)	0.08047 (**8.85%**)
	1.0027	0.894	0.03	0.07434	0.03402 (**13.38%**)	0.07915 (**6.47%**)	0.03310 (**10.33%**)	0.07434 (**5.03%**)
40	0.8459	0.513	0.03	0.04578	0.03526 (**17.53%**)	0.05530 (**20.77%**)	0.03279 (**9.29%**)	0.05222 (**14.05%**)
	0.8973	0.718	0.03	0.05597	0.03716 (**23.86%**)	0.06464 (**15.49%**)	0.03502 (**16.73%**)	0.06226 (**11.24%**)
	0.9507	0.785	0.03	0.05932	0.03496 (**16.54%**)	0.06572 (**10.79%**)	0.03335 (**11.16%**)	0.06409 (**8.04%**)
	1.0036	0.723	0.03	0.05786	0.03193 (**6.42%**)	0.06155 (**6.38%**)	0.03083 (**2.78%**)	0.06048 (**4.54%**)
60	0.8456	0.429	0.03	0.03773	0.03890 (**29.66%**)	0.04554 (**20.71%**)	0.03584 (**19.48%**)	0.04325 (**14.64%**)
	0.8975	0.527	0.03	0.04027	0.03935 (**31.15%**)	0.04670 (**15.97%**)	0.03642 (**21.39%**)	0.04474 (**11.10%**)
	0.9510	0.566	0.03	0.04058	0.03667 (**22.23%**)	0.04447 (**9.58%**)	0.03431 (**14.35%**)	0.04297 (**5.90%**)
	1.0036	0.552	0.03	0.03850	0.03263 (**8.76%**)	0.04037 (**4.84%**)	0.03089 (**2.98%**)	0.03928 (**2.02%**)
80	0.8460	0.244	0.03	0.02044	0.04099 (**36.62%**)	0.02451 (**19.94%**)	0.03913 (**30.44%**)	0.02392 (**17.04%**)
	0.8976	0.280	0.03	0.01938	0.03983 (**32.78%**)	0.02321 (**19.79%**)	0.03493 (**16.43%**)	0.02170 (**11.99%**)
	0.9505	0.339	0.03	0.01857	0.03558 (**18.58%**)	0.02097 (**12.94%**)	0.03197 (**6.57%**)	0.01987 (**7.03%**)
	1.0038	0.409	0.03	0.01749	0.03217 (**7.22%**)	0.01900 (**8.63%**)	0.02974 (**0.86%**)	0.01827 (**4.45%**)

Table 7
Comparison of experimental and analytical results in the pitching interaction of the structure and TLCD ($\nu = 3$)

Structure + TLCD ($\nu = 3$)								
			Experimental		Analytical			
					Without additional term		With additional term	
ψ (%) (1)	k (2)	$\hat{M}_0$ (3)	$\lvert\alpha_0\rvert$ (4)	$\lvert\hat{y}_0\rvert$ (5)	$\lvert\alpha_0\rvert$ (6)	$\lvert\hat{y}_0\rvert$ (7)	$\lvert\alpha_0\rvert$ (8)	$\lvert\hat{y}_0\rvert$ (9)
0	0.8476	0.900	0.03	0.04617	0.03090 (**3.00%**)	0.05200 (**12.61%**)	0.02914 (**2.86%**)	0.04944 (**7.06%**)
	0.8771	1.053	0.03	0.05238	0.03097 (**3.23%**)	0.05840 (**11.50%**)	0.02938 (**2.08%**)	0.05606 (**7.03%**)
	0.9386	1.325	0.03	0.06566	0.03357 (**11.88%**)	0.07189 (**9.49%**)	0.03206 (**6.87%**)	0.07004 (**6.67%**)
	0.9697	1.342	0.03	0.06891	0.03442 (**14.75%**)	0.07436 (**7.91%**)	0.03308 (**10.26%**)	0.07285 (**5.72%**)
20	0.8472	0.892	0.03	0.04539	0.03218 (**7.28%**)	0.05153 (**13.53%**)	0.03022 (**0.74%**)	0.04839 (**7.87%**)
	0.8771	1.025	0.03	0.05116	0.03242 (**8.05%**)	0.05670 (**10.82%**)	0.03059 (**1.97%**)	0.05438 (**6.29%**)
	0.9380	1.204	0.03	0.05991	0.03373 (**12.44%**)	0.06467 (**7.95%**)	0.03209 (**6.96%**)	0.06290 (**5.00%**)
	0.9689	1.187	0.03	0.06123	0.03323 (**10.76%**)	0.06481 (**5.85%**)	0.03181 (**6.04%**)	0.06338 (**3.51%**)
40	0.8479	0.823	0.03	0.04218	0.03402 (**13.41%**)	0.04723 (**11.99%**)	0.03157 (**5.25%**)	0.04482 (**6.26%**)
	0.8770	0.903	0.03	0.04487	0.03418 (**13.93%**)	0.04943 (**10.16%**)	0.03187 (**6.23%**)	0.04729 (**5.39%**)
	0.9381	0.968	0.03	0.04765	0.03332 (**11.06%**)	0.05058 (**6.16%**)	0.03140 (**4.65%**)	0.04901 (**2.84%**)
	0.9699	0.937	0.03	0.04708	0.03185 (**6.16%**)	0.04910 (**4.29%**)	0.03021 (**0.69%**)	0.04780 (**1.53%**)
60	0.8475	0.635	0.03	0.03172	0.03601 (**20.04%**)	0.03587 (**13.08%**)	0.03260 (**8.66%**)	0.03382 (**6.63%**)
	0.8773	0.665	0.03	0.03192	0.03500 (**16.68%**)	0.03528 (**10.52%**)	0.03190 (**6.33%**)	0.03350 (**4.93%**)
	0.9381	0.694	0.03	0.03137	0.03288 (**9.61%**)	0.03343 (**6.55%**)	0.03038 (**1.28%**)	0.03209 (**2.30%**)
	0.9691	0.691	0.03	0.03045	0.03153 (**5.08%**)	0.03206 (**5.29%**)	0.02933 (**2.23%**)	0.03092 (**1.53%**)
80	0.8468	0.352	0.03	0.01555	0.03862 (**28.82%**)	0.01839 (**18.26%**)	0.03259 (**8.65%**)	0.01683 (**8.26%**)
	0.8761	0.377	0.03	0.01505	0.03593 (**19.76%**)	0.01726 (**14.63%**)	0.03083 (**2.76%**)	0.01595 (**5.97%**)
	0.9374	0.456	0.03	0.01434	0.03336 (**11.18%**)	0.01572 (**9.61%**)	0.02970 (**1.02%**)	0.01483 (**3.39%**)
	0.9684	0.493	0.03	0.01387	0.03168 (**5.58%**)	0.01489 (**7.35%**)	0.02864 (**4.53%**)	0.01415 (**2.08%**)

the analytical responses with the additional term considered are smaller than the other. In other words, the analytical responses with the additional term considered are closer to the experimental responses. Therefore, the interacted dynamics of the TLCD and structure in the pitching direction can be better represented by including the additional term shown in Eq. (12) (or Eq. (14)).

6. Conclusions

The equation of motion for wind-induced interaction between a non-uniform TLCD and structure in pitching motion has been derived by means of energy principles, i.e., the approach of Lagrange's equations, and it was found that a term $-\rho g \nu A_h L_\nu^2 \alpha$ (see Eq. (12)), denoted as the additional term, has never been considered previously in the literature. The analytical solution of the interacted system subjected to harmonic load was also derived. Extensive simulation shows that in general the effect of the additional term becomes more significant when the horizontal length ratio p becomes smaller and the ratio of mass moment of inertia μ becomes larger. An experimental verification has been performed by conducting large scale tests of a TLCD on a rotational structure to demonstrate the existence of this additional term. Experimental results verify that the analytical responses with the additional term considered represent the interaction more closely than those without the additional term. Therefore, the inclusion of the additional term in the pitching interaction motion of a TLCD and structure is essential.

References

[1] Sakai F, Takaeda S, Tamaki T. Tuned liquid column damper-new type device for suppression of building vibration. In: Proc. int. conf. on high-rise building. 1989. p. 926–31.
[2] Xu YL, Samali B, Kwok KCS. Control of along-wind response of structures by mass and liquid dampers. ASCE J Eng Mech 1992;118(1):20–39.
[3] Hitchcock PA, Kwok KCS, Watkins RD. Characteristics of liquid column vibration absorbers (LCVA) — I, II. Eng Struct 1997;19:126–44.
[4] Balendra T, Wang CM, Rakesh G. Effectiveness of TLCD on various structural systems. Eng Struct 1999;21(4):291–305.
[5] Gao H, Kwok KCS, Samali B. Optimization of tuned liquid column damper. Eng Struct 1997;19(6):476–86.
[6] Chang CC, Hsu CT. Control performance of liquid column vibration absorbers. Eng Struct 1998;20(7):580–6.
[7] Chang CC. Mass dampers and their optimal designs for building vibration control. Eng Struct 1999;21:454–63.
[8] Wu JC, Shih MH, Lin YY, Shen YC. Design guidelines for tuned liquid column damper for structures responding to wind. Eng Struct 2005;27(13):1893–905.
[9] Kwon SD, Park KS. Suppression of bridge flutter using tuned mass dampers based on robust performance design. J Wind Eng Ind Aerodyn 2004;92(11):919–34.
[10] Pansare AP, Jangid RS. Tuned mass dampers for torsionally coupled systems. Wind Struct 2003;6(1):23–40.
[11] Jangid RS, Datta TK. Performance of multiple tuned mass dampers for torsionally coupled system. Earthq Eng Struct Dyn 1997;26(3):307–17.
[12] Xue SD, Ko JM, Xu YL. Tuned liquid column damper for suppressing pitching motion of structures. Eng Struct 2000;23(11):1538–51.
[13] Xue SD, Ko JM, Xu YL. Optimum parameters of tuned liquid column damper for suppressing pitching vibration of an undamped structure. J Sound Vibration 2000;235(4):639–53.
[14] Taflanidis AA, Angelides DC, Manos GC. Optimal design and performance of liquid column mass dampers for rotational vibration control of structures under white noise excitation. Eng Struct 2005;27(4):524–34.